

# Lab 3 Report

## 1 LCR Resonant Circuit

### 1.1 R-1: Falstad Simulation

To simulate the LCR resonant circuit, we used Falstad's circuit simulator. The component values were initially chosen as  $L = 50 \pm 1 \text{ mH}$ ,  $C = 10.3 \pm 0.1 \text{ nF}$ , and  $R = 100 \pm 1 \Omega$ , since:

$$f_0 = \frac{1}{2\pi\sqrt{(10.3 \times 10^{-9} \times 50 \times 10^{-3})}} = 7.013 \text{ kHz}$$

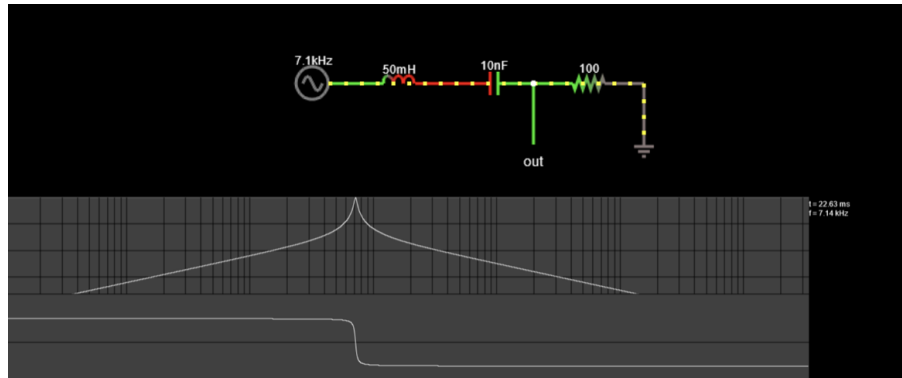


Figure 1: Falstad Simulation of LCR Circuit

### 1.2 R-2: Photo of Circuit

Below is an image of the circuit implementation on a breadboard.

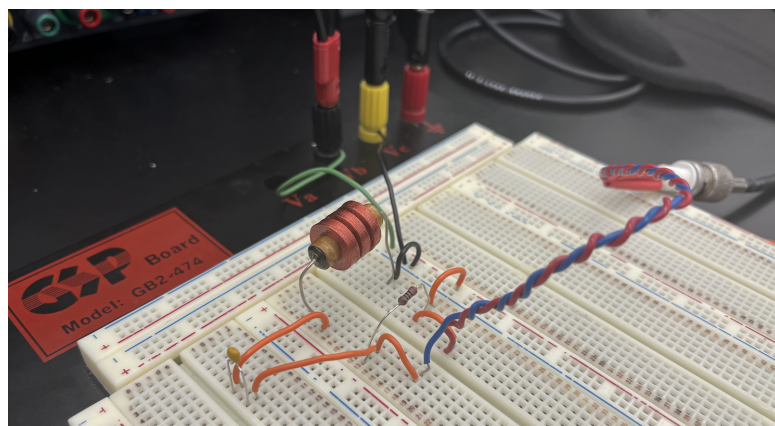


Figure 2: Breadboard implementation of the LCR circuit (initial configuration:  $L = 50 \text{ mH}$ ,  $C = 10.3 \text{ nF}$ ,  $R = 100\Omega$ ).

### 1.3 R-3: Bode Plot of Attenuation and Phase vs Frequency

The frequency response of the initial LCR circuit, where the output was measured across the resistor, is shown below:

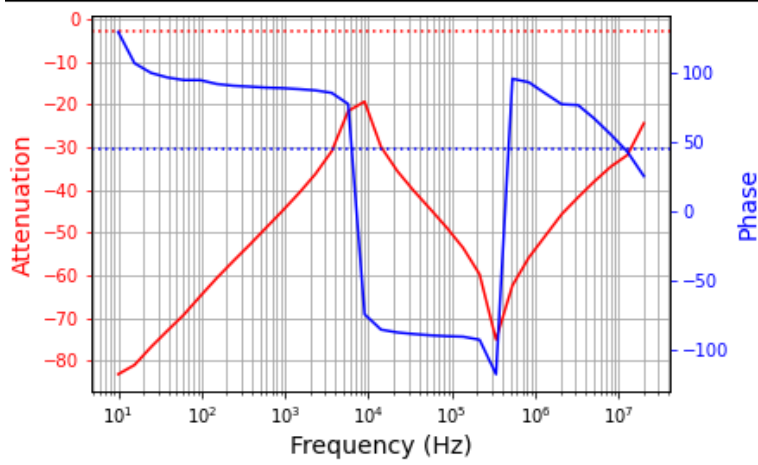


Figure 3: Bode plot of attenuation and phase vs frequency for initial LCR circuit.

### 1.4 R-4: Discussion of Previous Results

The peak attenuation was measured at approximately  $-19.32$  dB, which significantly exceeded the expected  $-4$  dB limit. The resonant frequency was found to be  $f_0 = 8.987$  kHz, which was significantly higher than the expected 7 kHz. We attempted to fix this by changing the capacitance to  $200\text{nF}$ , but the resonance frequency remained at  $f_0 = 8.987$  kHz, indicating that the inductor was dominating the behaviour of the circuit.

Furthermore, there appeared to be a second resonance somewhere around the  $f = 10^7$  mark, which could indicate a secondary resonance due to the inductor's self-resonance frequency (SRF). This would mean the parasitic capacitance was:

$$C_p = \frac{1}{L(2\pi f_0)^2} = \frac{1}{(3.3 \times 10^{-3})(2\pi(10^7))^2} \approx 7.68 \times 10^{-14} F$$

but this is unrealistically small for an inductor of the size we used. Ultimately, since both the attenuation and resonant frequency exceeded the required specifications, we modified the component values to  $L = 3.3 \pm 0.1$  mH,  $C = 156 \pm 2$  nF, and  $R = 15 \pm 1$   $\Omega$ . (It is worth noting that while we couldn't find a  $150\text{nF}$  capacitor, we used a  $\approx 100\text{nF}$  and  $\approx 50\text{nF}$  one in parallel, which, measured using a multimeter rendered a net capacitance of  $C = 156 \pm 2$  nF).

Combined, these still rendered a theoretical resonant frequency of around 7kHz:

$$f_0 = \frac{1}{2\pi\sqrt{(156 \times 10^{-9} \times 3.3 \times 10^{-3})}} = 7.014\text{kHz}$$

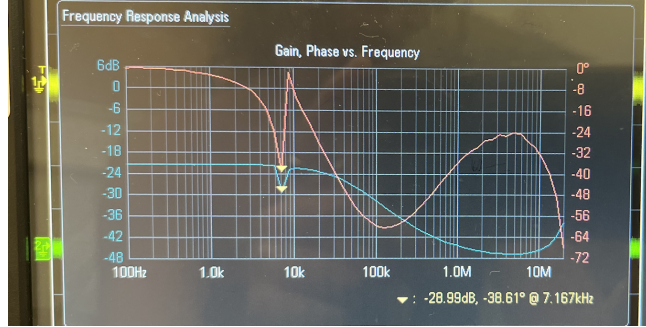


Figure 4: Bode plot of attenuation and phase vs frequency for modified LCR circuit.

Using these R-C values, we were able to achieve a much better resonance frequency of  $f_0 = 7.167$  kHz, which is extremely close to the predicted resonance, and is within  $7 \pm 1$  kHz, as desired. However, these modifications unfortunately made the attenuation values worse than before, reaching  $-28.99\text{dB}$ .

## 1.5 R-5: Measuring the Output Across the Inductor and Capacitor

Continuing with the modified LCR circuit from before, we tested the output across the inductor and capacitor using an initial capacitance of  $156\text{nF}$ .

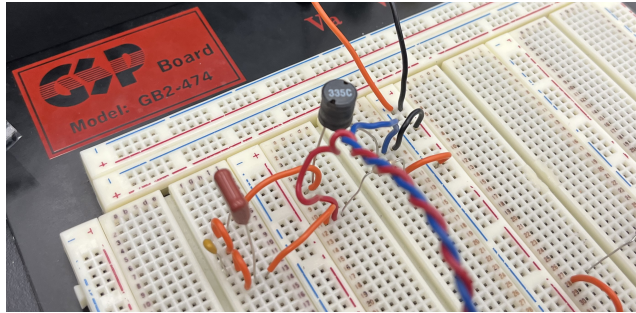


Figure 5: LCR circuit with  $L = 3.3$  mH,  $C = 156$  nF,  $R = 100$   $\Omega$ .

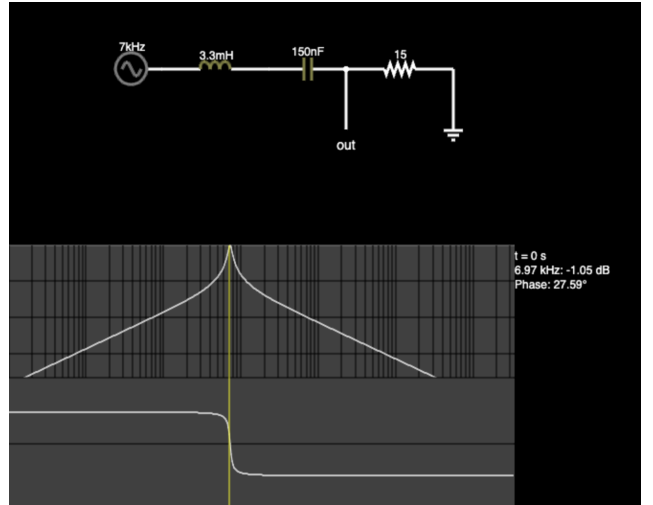


Figure 6: Falstad simulation using new R-C values.

Despite the RC values predicting a resonance at  $f_0 = 7.014$  kHz, the resonance peak was at  $f_0 \approx 5.7$  kHz. This was despite having verified the capacitance using the multimeter, indicating the issue came from elsewhere.

Since the capacitance values were verified using a multimeter (using alligator clips directly on the circuit), this suggests that the issue lies elsewhere in the circuit behavior rather than inaccurate capacitor values.

Potential reasons for the mismatch between the theoretical and experimental resonant frequency could be that the inductor's actual inductance may not be precisely 3.3 mH due to manufacturing tolerances, causing deviations in  $f_0$ . Furthermore, the breadboard's parasitic capacitance could have affected the circuit in an unpredictable way, altering the resonance conditions. Since these are parallel capacitances, and parallel capacitances add, the net capacitance was likely higher than expected, contributing to the smaller 5.711 kHz resonance we measured.

## 2 I-V Characteristics of a Diode

### 2.1 R-6: Comparing Exponential Model to Experimental I-V Curve

The I-V characteristics of a standard diode follow an exponential relationship given by:

$$i = i_s \left( e^{\frac{eV}{k_B T}} - 1 \right)$$

where  $i_s$  is the reverse saturation current,  $e$  is the electron charge,  $k_B$  is the Boltzmann constant, and  $T$  is the temperature of the diode.

To test this model, we measured the current flowing through the blue LED as a function of applied voltage in the forward direction. A log plot of the measured current versus voltage is shown in Figure 7. The trendline suggests that the current follows an approximately exponential behavior, with some deviation at higher voltages due to resistive effects in the diode.

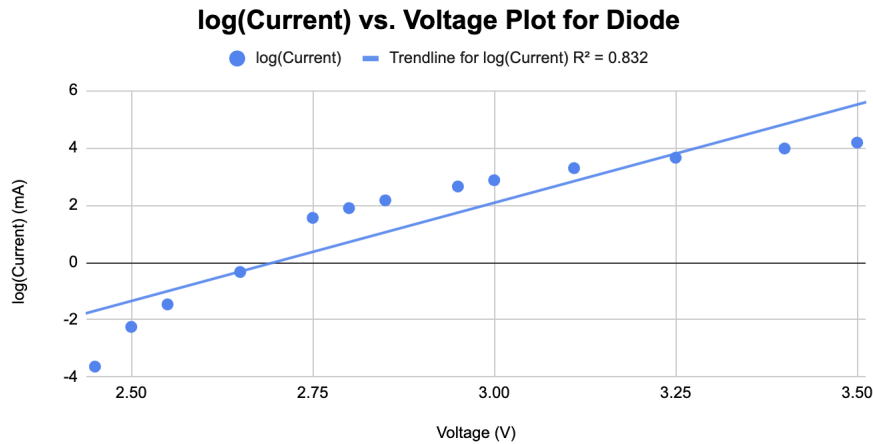


Figure 7: Log(Current) vs. Voltage plot for the blue LED. The linearity on the semilog plot suggests agreement with the exponential diode equation.

The plot confirms that the diode's forward current follows an exponential trend with voltage, consistent with the diode equation. The deviation at higher currents can be attributed to series resistance in the LED.

### 2.2 R-7: Display for Zener Diode

To observe the I-V characteristics of a zener diode, we connected it in series with a  $1\text{k}\Omega$  resistor and applied a ramp voltage.



Figure 8: Oscilloscope display of voltage across resistor (proportional to current) vs. voltage across both resistor and zener diode.

The forward-biased region (right side of the plot) shows an exponential increase in current, similar to a regular diode. However, in the reverse-biased region (left side), the zener breakdown voltage is evident. At a sufficiently high reverse voltage (approximately 3.9V), the diode begins conducting in reverse, stabilizing the voltage.

It is important to note that this display does not directly give the I-V curve of the zener diode. As our professor pointed out, the oscilloscope is plotting *voltage across the resistor* (proportional to current) vs. *voltage across both the diode and resistor*. To obtain the actual I-V curve, we would need to plot:

$$(V_{\text{total}} - V_R) \quad \text{vs} \quad \left( \frac{V_R}{R} \right)$$

where  $V_{\text{total}}$  is the applied voltage and  $V_R$  is the voltage drop across the resistor. This correction would produce a more accurate representation of the zener diode's electrical behavior.

### 3 AC-to-DC Power Supply

#### 3.1 R-8: Rectifier Circuit Analysis

To convert an AC signal to DC, we implemented a rectifier circuit using a 1N4001 rectifier diode, a 3.9V Zener diode, a  $470\mu\text{F}$  capacitor for smoothing, and an RC low-pass filter with  $100\Omega$  and  $330\mu\text{F}$  to further refine the output voltage. The circuit was designed to take a 20Vpp, 60Hz square-wave input and output approximately 3.9V DC across a  $1\text{k}\Omega$  load resistor, with ripple minimized to under 5%, as shown in the Falstad simulation.

The rectifier diode was placed in series with the AC source to allow only positive half-cycles to pass, effectively rectifying the signal. The  $470\mu\text{F}$  capacitor was positioned in parallel with the load resistor, acting as a smoothing capacitor to reduce ripple. Additionally, a  $100\ \Omega$  resistor was placed in series, and a  $330\mu\text{F}$  capacitor was added in parallel to form an RC low-pass filter, further reducing AC variations in the output.

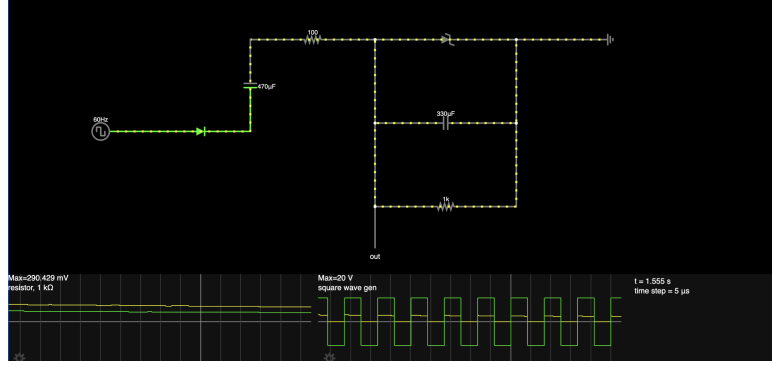


Figure 9: Falstad simulation of the rectifier circuit, confirming expected behavior.

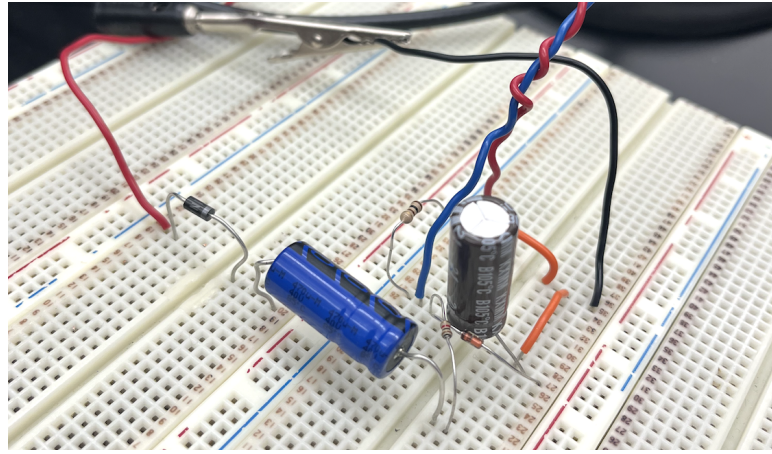


Figure 10: Breadboard implementation of the rectifier circuit.

From our oscilloscope measurements, we observed that the rectified output closely followed the expected waveform (based on the simulation), with a significant reduction in ripple due to the large capacitor values in the filtering stage. We also noticed that increasing the capacitance in the RC filter led to a more stable DC voltage, which is expected, as a larger RC time constant ( $\tau = RC$ ) ensures better attenuation of high-frequency ripples. The final waveform on the oscilloscope confirmed a steady DC output.



Figure 11: Scope output of rectified signal.



Figure 12: Centering the signals for comparison.